ARCHITECTURE CIVIL ENGINEERING ENVIRONMENT
The Silesian University of Technology No. 2/2024

doi: 10.2478/ACEE-2024-0014

ADVANCED AI TOOLS FOR PREDICTING MECHANICAL PROPERTIES OF SELF-COMPACTING CONCRETE

Achal AGRAWAL [a], Narayan CHANDAK [b*]

[a] Research Scholar; MPSTME NMIMS (Deemed to be University), Mumbai, India
Assistant Prof.; Department of Civil Engineering, SVKMs Institute of Technology, Dhule, India
E-mail address: *achalagrawal031@gmail.com*

[b] Prof.; Department of Civil Engineering, SVKMs Institute of Technology, Dhule, India
ORCID 0000-0002-4211-0828
*Corresponding author. E-mail address: *narayan.c@svkm.ac.in*

Received: 25.10.2023; Revised: 8.01.2024; Accepted: 25.01.2024

Abstract
The present study utilizes advanced numerical evaluation techniques like Artificial Intelligence (AI), including Support Vector Machines (SVM), Artificial Neural Networks (ANN), Adaptive Neuro-Fuzzy Inference Systems with Genetic Algorithms (ANFIS-GA), Gene Expression Programming (GEP), and Multiple Linear Regression (MLR) to develop and compare the predictive models for determination of compressive and tensile strength. Partial mutual information for selection and establishment of the degree of association of variables was used to aid in better attainment of results obtained through predictive models. It was observed that amongst the modeling techniques, the results obtained for compressive strength through the SVM technique were excellent, producing an Index of Agreement of 0.96, Akaike Information Criterion of 68.33, skill score of 0.96, and symmetric uncertainty of 0.93, thus indicating a simpler, robust, and low uncertainty predictive model. Furthermore, the adapted technique MLR was found to predict tensile strength characteristics better, with the MLR model demonstrating a higher R^2 value of 0.81, thus implying a reliable tensile strength prediction model. However, SVM consistently performed well for both compressive and tensile strength characteristics thus endorsing the reliability of the predictive model. Overall, the study aids in getting new insights about improvising the strength properties of SCC and its evaluation through predictive techniques.

Keywords: **Artificial Intelligence; Compressive strength; Support vector machines; Self-Compacting Concrete; Tensile strength.**

1. INTRODUCTION

SCC stands as a pioneering development in the construction industry, prominent for its intrinsic self-flowability into formwork and eliminating the requirement of mechanical vibration. Its attributes comprise uniform placement, compaction without segregation, enduring mechanical properties, enhanced early-age strength, greater toughness, improved volume stability, and extended service life. SCC offers unparalleled flexibility and simplicity in construction methodologies [1, 2]. SCC primarily consists of conventional concrete materials VIZ cement, coarse aggregates, fine aggregates, and water. However, to enhance the overall workability, strength, and durability properties of SCC, different additives are used, such as chemical admixtures, mineral admixtures, and fibers [3]. To achieve the desired properties, SCC formulation success depends on a meticulous mix design process. Boukendakdji et al. [4] suggested that maintaining balance in cement, aggregate types, and additives is crucial to ensure the robustness and efficiency of SCC that may arise due to variability caused during the production process. Due to its self-venting capabilities, SCC frequently exhibits superior performance,

making it appropriate for reinforcing and strengthening reinforced concrete beams [5, 6]. Despite its widespread use, designing an optimal SCC mixture remains challenging. This complexity is attributed to the quasi-brittle nature of concrete [7], as SCC requires precise flow characteristics. To enhance its properties, industrial waste by-products such as fly ash, silica fume, and ground granulated blast furnace slag (GGBFS) are often added to the cementitious system [8]. Incorporating these waste materials as partial replacements for cement has been shown to significantly reduce energy consumption and CO_2 emissions, contributing to sustainable construction practices [9]. Fly ash has significant pozzolanic characteristics, principally including Al_2O_3 and SiO_2. Fly ash must fulfill particular requirements and conformance criteria to be used in concrete manufacturing [10]. For the mix design process, secondary ingredients such as limestone powder, fly ash, GGBFS, silica fumes, rice husk ash (RHA), and, as chemical admixtures, next-generation SP and viscosity-modifying admixtures (VMA) were used [4, 11, 12]. The superplasticizer content is a critical factor that imparts high flowability to SCC by reducing its viscosity and enhancing workability. [13] The powder content, which consists of cement and supplementary cementitious materials such as fly ash or GGBFS, plays a fundamental role in determining the strength and durability of the SCC [14]. Concrete needs water to hydrate, but as a result of temperature fluctuations, the water evaporation process occurs, causing the concrete to self-desiccate and undergo autogenous shrinkage. Internal curing using materials like hydrophilic chemicals, lightweight aggregate (LWA), and super-absorbent polymers (SAPs) produces special concretes with superior performance, but conventional curing methods are unable to address this issue [15, 16, 17]. To increase the curing efficiency of SCC, the study looked into the function of hydrophilic and hydrophobic chemicals as self-curing compounds [18]. The inclusion of polypropylene and steel fibers is often used to improve the tensile strength and crack resistance of the concrete [19].

AI techniques have become practical tools in recent years for predicting the strength of SCC and facilitating effective mix design procedures. Advanced machine learning algorithms and computational models are used as an AI technique to predict the strength of SCC. These methods create intricate connections between input variables and the compressive strength of SCC by utilizing the power of data-driven analysis. The composition of cement, fly ash, ground granulated blast furnace slag, water-to-binder ratio, superplasticizer dosage, and the presence of fibers may all be important factors in predicting SCC strength [20, 21]. ANNs, modeled after the human brain's neural connections, are one widely used AI technique. ANNs can successfully handle nonlinear relationships and capture the intricate interactions between input parameters and SCC strength [20, 21]. Support Vector Regression (SVR), which excels at managing complex data distributions and delivering trustworthy results, is another AI technique used in SCC strength prediction [22].

Additionally, a versatile AI method called genetic programming (GP) is used to develop mathematical expressions that simulate the relationship between input parameters and SCC strength [23]. GP uses evolutionary algorithms to iteratively improve mathematical models, improving the predictions based on experimental and historical data. There are several benefits to using AI methods to predict SCC strength. First, it speeds up the mix design procedure and eliminates the need for time-consuming, expensive experimental trials. Second, AI models can easily handle sizable datasets, incorporating various parameters that influence SCC strength, resulting in thorough analysis and more precise predictions [14, 24].

Additionally, careful selection of the AI technique and appropriate parameterization is crucial to avoid overfitting or underfitting the data [24, 25]. Pallapothu et al. [26] suggested that particle packing models and machine learning may be used to estimate and optimize the packing density of the concrete mixture. Further, data obtained through the estimation was used as input in a machine-learning model. The findings suggested that the developed method performs better than conventional empirical models in precisely forecasting the compressive strength of concrete based on packing density and does away with the necessity for experimenting with various mix proportions.

This study investigates the influence of superplasticizer content, powder content, polypropylene, and steel fiber content on the strength characteristics of SCC. Further, the research focuses on predicting the compressive strength and tensile strength of SCC using various AI techniques, such as GEP, ANFIS-GA, SVM, ANN, and MLR. This multi-technique AI approach aids in creating a reliable prediction model for estimating SCC strength characteristics with proficiency. One of the novel aspects the current study holds is the dual prediction of compressive and tensile strength, which enables a thorough analysis of the material's mechanical properties. Additionally, the study employs PMI for input variable selection (IVS)

to guarantee that the most critical parameters are included. This novel method increases the precision of the predictive models by identifying the key factors influencing SCC strength. The research also uses several evaluation metrics, including the index of agreement (IOA), root mean square error (RMSE), mean absolute percentage error (MAPE), skill score (SS), correlation (Correl), and Taylor diagram, to fully assess the performance of the AI models. The models also go through rigorous calibration and validation procedures for optimal performance and generalizability of new data. The research builds on existing knowledge, identifies gaps in the current understanding, and establishes a solid framework for the study.

2. MATERIALS AND METHODS

The materials included cement, powder content, PP fiber, steel fiber, and several other parameters relevant to SCC performance. Multi-technique AI approaches, including GEP, ANFIS-GA, SVM, ANN, and MLR, are employed to ensure comprehensive analysis. A novel IVS method using PMI was utilized for selecting the most significant parameters. Evaluation metrics such as IOA, RMSE, MAPE, SS, Correl, and Taylor diagrams are used to assess the AI models' performance. Rigorous calibration and validation processes were carried out to enhance model accuracy and generalizability. The datasets for various techniques used in this paper are normalized against their maximum values, as shown in Table 1. The data has been divided into two groups: a) training dataset – required to build a model. In this study, 58 test results (80% of the total data) are used for training data and b) a testing dataset, which is required to estimate the performance of the model. The remaining, i.e., 14 test results (20% of the total data), are considered testing data. The research contributes to optimizing SCC for sustainable construction practices.

2.1. Methods

Multi-Technique AI Approach: In the present study, multiple AI techniques, including GEP, ANFIS-GA, SVR, ANN, and MLR, are used. This diverse approach allowed for a thorough analysis and comparison of the predictive capabilities of different AI algorithms. Where SP is superplasticizer, PC is powder content that constitutes cement and fly ash, PPF is polypropylene fiber, SF is steel fiber, FA is fine aggregate, and CA1 and CA2 are coarse aggregates, respectively. In addition to constituents, the representation of test results is depicted as SFD for slump flow diameter, SFT for slump flow time, VF for V-funnel testing time, CS28 for compressive strength after 28 days, and TS28 for tensile strength after 28 days.

Table 1.
Dataset for training and testing of different models

SP (kg)	PC (kg)	PPF (kg)	SF (kg)	SFD (Dia)	SFT (Sec)	VF (Sec)	CS28 (MPa)	TS28 (MPa)	Water (kg)	FA (kg)	CA1 20-10 mm (kg)	CA2 10-4.75 mm (kg)
9	600	0	0	780	2	7	36.11	4.41	240	810	365	365
9	600	1.5	3	665	5	13	39.95	4.79	240	810	365	365
9	600	3	6	630	6	14	41.1	5.26	240	810	365	365
9.225	615	0	0	790	1.5	6	39.55	4.67	246	810	365	365
9.225	615	1.535	3.07	730	3	9	42.33	5.66	246	810	365	365
9.225	615	3.07	6.15	690	4	11	46.31	6.12	246	810	365	365
9.45	630	0	3.15	750	2.5	8	45.52	6.03	252	810	365	365
9.45	630	1.575	6.3	730	3	8	49.16	6.88	252	810	365	365
9.45	630	3.15	0	725	3	9	46.46	6.28	252	810	365	365
12	600	0	6	760	2	8	44.12	5.86	240	810	365	365
12	600	1.5	0	765	2	7	41.68	5.53	240	810	365	365
12	600	3	3	710	4	12	45.09	6.22	240	810	365	365
12.3	615	0	3.07	775	2	7	48.03	6.74	246	810	365	365
12.3	615	1.535	6.15	725	3	9	53.11	7.26	246	810	365	365
12.3	615	3.07	0	710	4	10	47.36	6.67	246	810	365	365
12.6	630	0	6.3	810	1	6	57.16	7.8	252	810	365	365
12.6	630	1.575	0	785	2	6	54.3	7.52	252	810	365	365
12.6	630	3.15	3.15	750	3	9	56.44	7.76	252	810	365	365
3.3	565	0	0	690	2	11	52.8	3.9	186	750	58.5	391.5

→

SP (kg)	PC (kg)	PPF (kg)	SF (kg)	SFD (Dia)	SFT (Sec)	VF (Sec)	CS28 (MPa)	TS28 (MPa)	Water (kg)	FA (kg)	CA1 20-10 mm (kg)	CA2 10-4.75 mm (kg)
5	566.7	0	0	680	2.2	16	57.3	4	170	760	58.5	391.5
5.1	566.7	0	39	665	2.8	18	56.9	5.9	170	760	58.5	391.5
5.3	566.7	4.55	39	670	3.1	19	61.7	6.9	170	760	58.5	391.5
5.7	566.7	6.825	39	660	3.3	18	58.8	7.2	170	760	58.5	391.5
6.2	566.7	9.1	39	645	4.2	20	56.7	6.9	170	760	58.5	391.5
10	500	0	0	700	2.4	7	37.21	4.25	190	1005	310	310
10	500	0	157	600	4	12	51.31	7.2	190	1005	310	310
10	500	0	117.75	620	3.8	11	50.24	6.25	190	1005	310	310
10	500	0	78.5	640	3.5	10.5	50.45	6.1	190	1005	310	310
10	500	0	39.25	650	3.5	10.5	45.64	4.8	190	1005	310	310
10	500	0	0	670	3	8.3	34.87	4.1	190	1005	310	310
10	500	0.455	157	580	5	12.7	40.52	5.8	190	1005	310	310
10	500	0.455	117.75	600	4	12	45.78	5.8	190	1005	310	310
10	500	0.455	78.5	620	3.5	11	50.44	6.25	190	1005	310	310
10	500	0.455	39.25	630	3.5	10.6	47.86	5.85	190	1005	310	310
10	500	0.455	0	640	3.2	10.5	47.84	5.75	190	1005	310	310
10	500	0.91	157	560	5.5	13	64.1	7.25	190	1005	310	310
10	500	0.91	117.75	570	5.5	12.5	54.98	6.15	190	1005	310	310
10	500	0.91	78.5	590	5	11.5	47.64	5.7	190	1005	310	310
10	500	0.91	39.25	610	4.5	11	46.09	5.75	190	1005	310	310
10	500	0.91	0	620	4	11	43.96	3.8	190	1005	310	310
10	500	0	0	720	2.2	6.8	39.04	4.3	190	1005	310	310
10	500	0	157	620	4	11.6	66.69	7.95	190	1005	310	310
10	500	0	117.75	630	4	11	53.91	6.5	190	1005	310	310
10	500	0	78.5	640	3.5	10.5	52.31	6.5	190	1005	310	310
10	500	0	39.25	660	3.5	10.5	47.96	5.7	190	1005	310	310
10	500	0	0	680	2.5	8.1	39.53	4.6	190	1005	310	310
10	500	0.455	157	600	4.5	12.5	52.27	6.45	190	1005	310	310
10	500	0.455	117.75	620	4	12	62.67	7.35	190	1005	310	310
10	500	0.455	78.5	630	4	11	56.92	6.5	190	1005	310	310
10	500	0.455	39.25	640	3.5	10.4	55.13	6.45	190	1005	310	310
10	500	0.455	0	650	3.5	10.2	53.21	6.2	190	1005	310	310
10	500	0.91	157	580	5.5	12.5	69.12	8.1	190	1005	310	310
10	500	0.91	117.75	590	5.5	12	55.68	6.8	190	1005	310	310
10	500	0.91	78.5	600	5	11.8	50.05	6.4	190	1005	310	310
10	500	0.91	39.25	620	4	11	46.5	5.9	190	1005	310	310
10	500	0.91	0	630	4	10.6	46.05	4.4	190	1005	310	310
10	500	0	0	740	2	6.8	42.83	4.95	190	1005	310	310
10	500	0	157	630	4	11.6	68.14	8.05	190	1005	310	310
10	500	0	117.75	630	4	11	64.79	7.5	190	1005	310	310
10	500	0	78.5	650	3.2	10.5	56.55	6.65	190	1005	310	310
10	500	0	39.25	660	3	10.5	49.82	5.9	190	1005	310	310
10	500	0	0	700	2.5	8.1	46.72	4.75	190	1005	310	310
10	500	0.455	157	620	4.5	12.5	60.22	7	190	1005	310	310
10	500	0.455	117.75	630	4	12	69.71	8.15	190	1005	310	310
10	500	0.455	78.5	640	4	11	64.52	7.4	190	1005	310	310
10	500	0.455	39.25	650	3.5	10.4	56.7	6.6	190	1005	310	310
10	500	0.455	0	670	3	10.2	53.73	6.55	190	1005	310	310
10	500	0.91	157	600	5	12.5	69.79	8.15	190	1005	310	310
10	500	0.91	117.75	610	5	12	56.67	7.75	190	1005	310	310
10	500	0.91	78.5	620	4.5	11.8	52.48	6.8	190	1005	310	310
10	500	0.91	39.25	640	3.5	11	49.6	6.15	190	1005	310	310
10	500	0.91	0	650	3.5	10.6	49.4	5	190	1005	310	310

2.2. Gene Expression Programming

There are five essential phases to employing GEP [27]. The first and most critical stage in any modeling process is data preparation. The outlier approach may be used to assess data quality. If an outlier is discovered, it may be deleted. GEP necessitates specifying the predictors and outcomes for the modeling. In this study, predictors were the parameters influencing SCC strength (compressive and tensile), such as superplasticizer (kg), powder content (kg), polypropylene fibre (kg), steel fibre (kg), slump flow diameter (Dia.), slump flow time (sec), J-ring (mm), V-funnel (sec), and so on, and predictors were compressive and tensile strength [20]. The next step is to choose a fitness function and a starting population. The present research used multigenic chromosomes (composed of three genes). In the initial population, any number of population sizes can be used; it is inferred that chromosomes in the range of 30–100 have yielded promising results. Based on trials, a population size of 30 chromosomes was chosen as the optimal size and used in all GEP models.

For the present problem, the fitness fi of an individual program 'i' is evaluated using Eq. 1:

$$f_i = \sum_{i=1}^{c_t}(M - |C_{ij} - T_j|) \quad (1)$$

Where, M – data range, $C_{i,j}$ – value returned by the individual chromosome "i" for fitness case "j", and T_j – target value for fitness case j.

Other parameter descriptions for the model development are given in Table 1. The significant fourth step is to choose the linking function as multiplication. The last step is to select the set of genetic operators. A combination of all operators, i.e., mutation, transposition, and crossover, are used for this purpose, as shown in Table 2. Once all the parameters are added to the algorithm, the combination of different genes and chromosomes is processed to evaluate the data fit, and a model that satisfies the fitness criteria will be printed, followed by algorithm termination.

Table 2.
GEP parameters [27]

Parameters	Values
Population size	30
Genes per chromosome	3
Gene head length	9
Functions	+, -./, *, ^
Gene tail length	12
Mutation rate	0.05
Inversion rate	0.1
Gene transposition rate	0.1
One-point recombination rate	0.3
Two-point recombination rate	0.3
Gene recombination rate	0.1
Fitness function	R ≥ 0.7

2.3. Adaptive Neuro-Fuzzy Inference System with Genetic Algorithm

The ANFIS-GA algorithm starts with generating a fuzzy inference system using the Takagi-Sugeno-Kang (TSK) fuzzy model. The initial values of ANFIS-GA parameters are presented in Table 3. The fuzzy system involves a set of rules defining linguistic relationships between variables (input and output). Each rule consists of precursor and resulting parts. The precursor part utilizes linguistic terms to represent the input variables' fuzzy sets, while the consequent part comprises linear functions involving the output or resulting variables. Next, hybridization with neural networks takes place, where the parameters of the fuzzy inference system are tuned using a learning algorithm based on the backpropagation method. The neural network component must alter the membership functions and coefficients of linear functions to lessen the discrepancy between the predicted and actual SCC strengths [13, 28, 29]. The ANFIS network and its many layers are used for modeling and learning. The model can adjust its parameters based on the training data. A genetic algorithm is used to improve the ANFIS-GA model even more. The best individuals are chosen for reproduction by the genetic algorithm, which assesses the fitness of each candidate solution based on how well it predicts the training data, causing the population to evolve towards more ideal solutions. Once the ANFIS-GA model shown in Fig. 1 is trained and optimized, it can be used to predict the strength of SCC for the new input data. The model's ability to capture complex nonlinear relationships and its adaptive nature provide accurate and reliable predictions for various SCC compositions and properties.

Table 3.
Initial values of ANFIS GA parameters [28]

Parameters	Values
Population size	20
Iterations	1000
Crossover rate	0.70
Mutation rate	0.50
Inversion rate	0.10
Selection pressure	8.0
Gamma	0.20

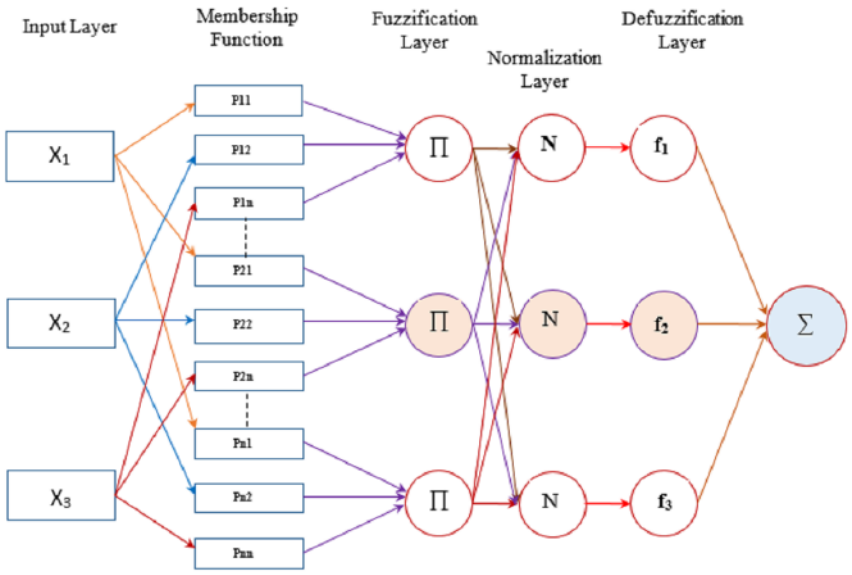

Figure 1.
ANFIS network designed for the SCC strength modeling [28]

2.4. Support Vector Regression

The concept of SVM, developed by [30], involves using mathematical principles to create predictive models. [31] outlined the diverse applications, highlighting how SVM had been utilized to address challenges such as structural integrity assessment, vibration analysis, and load prediction refer to Fig. 2.

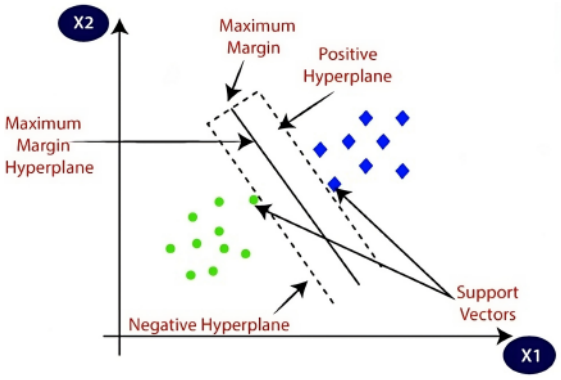

Figure 2.
Hyperplanes of SVR [30]

Saha P. et al. [23] discussed the SVR capabilities of the SCC. By accurately modeling the relationships between the parameters and the mechanical strengths, we aim to provide an efficient and reliable tool for estimating SCC's compressive and tensile properties. A quadratic programming problem with linear constraints is used as the kernel function with SVM for defining network weights. This approach is an alternative training method to a radial basis function, multi-layer perceptron, and polynomial classifiers [20]. Mathematically, SVM can be expressed as given by Eq. 2.

$$f(x, a_i, a_i^*) = \sum_{i=1}^{n} (a_i - a_i^*) M(x_i, x_j) + b \qquad (2)$$

Where, a_i and a_i^* – positive Lagrange multipliers and $M(x_i x_j)$ – a non-linear transformation using linear kernel function of SVM, and b – "bias". Radial Bias Function (RBF) kernels are well suited for the SCC modeling around a bridge pier [20]. The configuration set to predict the SCC model is shown in Table 4.

Table 4.
SVM parameters used in the present study [20]

SVM Parameter	Adoption/Values
Kernel function	RBF
Scaling factor	1
Method	Quadratic programming
Support Vectors	13 x 5
Bias	-0.012

2.5. Artificial Neural Networks

By utilizing multiple layers of interconnected nodes, ANNs, as shown in Fig. 3, are capable of discerning underlying relationships within the parameter space. This facilitates accurate predictions of compressive and tensile strength of SCC [10, 19, 20, 23].

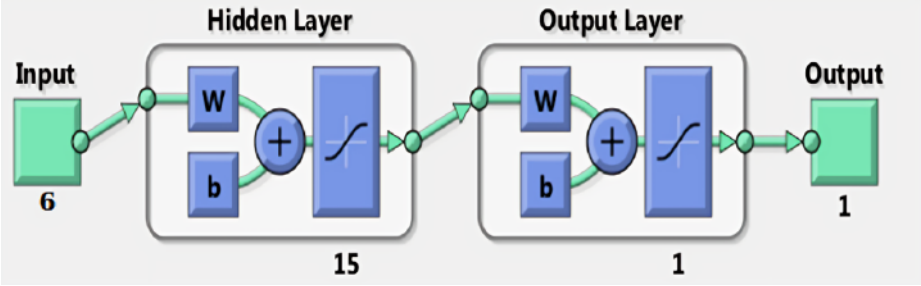

Figure 3.
ANN architecture [23]

2.6. Statistical Metrics

For the evaluation of model performances, evaluation criteria (EC) such as IOA, RMSE, Akaike information criterion (AIC), SS, and Symmetric Uncertainty (SU) were employed in the present study. The following section briefly describes EC.

2.6.1. Index of Agreement

It is the ratio of the mean square error and the potential error given in Eq. 3. The degree of model prediction error varies between "0" and "1". The agreement value of "1" indicates a perfect match, and "0" indicates no agreement. The index of agreement can detect additive and proportional differences in the observed and simulated means and variances.

$$IOA = 1 - \frac{\sum_{i=1}^{n}(O_i - P_i)^2}{\sum_{i=1}^{n}(|P_i - \bar{O}|) + (|O_i - \bar{O}|)^2} \tag{3}$$

RMSE can be expressed as given by Eq. 4:

$$RMSE = \sqrt{\frac{1}{N}\sum_{i=1}^{n}(O_i - P_i)^2} \tag{4}$$

Where, O – observed compressive strength and P – predicted compressive strength.

2.6.2. Akaike Information Criterion

Negative AIC values indicate better performance of the proposed model compared to positive ones. Eq. 5 is the mathematical expression of AIC.

$$AIC = N \ln (N.RMSE^2)\ 2NOV \tag{5}$$

Where, N – size of observations; and NOV – independent variables (nos.).

2.6.3. Skill Score (SS)

It was proposed by Amstrong N. et al, [32] which allows comparison across the entire probability density functions (PDFs), and is expressed as Eq. 6.

$$SS = \sum_{i=1}^{nb} \min (f_m, f_o) \tag{6}$$

Where, *nb* – number of bins used to calculate the PDFs for a given region, f_m – frequency of values in the given bin, and f_o – frequency of values in the given bin from the observed data. Based on the score we can categorize whether the model simulates perfectly i.e., SS close to "1" or the model simulates the observed condition poorly if the score is close to "0".

2.6.4. Symmetric Uncertainty

SU uses mutual information (MI) to assess the association between the two. If p(A) and p(B) are the probability density functions and p(A, B) is the joint probability density function of A and B, then MI between A and B is Eq. 7:

$$MI(A,B) = \sum p(A,B) log \frac{p(A,B)}{p(A).p(B)} \tag{7}$$

MI estimates common information between two variables as the difference between the sum of the entropies and their joint entropy Eq. 8:

$$\mathrm{MI(A,B)} = \mathrm{H\ (A)} - \mathrm{H(A,B)} \tag{8}$$

Where H (A) and H (A, B) denotes Shannon's entropy of "A" and the joint entropy of "A" and "B", respectively, the MI estimated using Eq. (8) indicates the mutual information between observed and predicted compressive strength. Independent variables indicate MI as zero, while a higher value of MI indicates the predicted compressive strength has a higher similarity with the observed compressive strength. The MI is biased towards the variable having higher values. This can be overcome using SU, where the estimated MI is divided by the total entropies of observed and predicted compressive strength as

given by Eq. 9:

$$SU(A,B) = 2\frac{MI(A,B)}{H(A) + H(B)} \quad (9)$$

SU value "1" means a complete agreement between observed and predicted compressive strength, while "0" indicates no agreement.

2.6.5. Partial Mutual Information

PMI assists in identifying the SCC parameters that have the most considerable effects on the compressive and tensile strengths. A key element of PMI, MI, is calculated using Shannon entropy Eq. 10, which measures how random or uncertain a variable's distribution is. For two random variables X and Y, the mutual information can be calculated as:

$$[I(X;\ Y) = H(X) + H(Y) - H(X,Y)] \quad (10)$$

Where, H(X) – Shannon entropy of variable X, H(Y) – Shannon entropy of variable Y, H(X, Y) – joint Shannon entropy of variables X and Y.

The joint Shannon entropy H(X, Y) is computed using the joint probability density function Eq. 11:

$$H(X) = -\int f_x(x) ln f_x(x) dx$$
$$H(Y) = -\int f_y(y) ln f_y(y) dy \quad (11)$$
$$H(X,Y) = -\iint f_{X,Y}(x,y) ln(x,y) dx dy$$

It introduces a third variable, Z, to account for its influence on the relationship between X and Y. Let X_i (i=1, 2….) be the potential inputs for time series prediction, Y the output, and Si the selected set of I inputs. So, it represents an empty set – the PMI between the output Y and the potential input X_i with a selected set of inputs Si. The PMI between X and Y giving Z is given by Eq. 12 [33].

$$H(X) = -E(lnf(X)) =$$
$$-\sum_{i=1}^{N} \ln\left(\frac{1}{N(2\lambda)^d}\right) \sum_{j=1}^{N} \exp\left(-\frac{1}{\lambda}\sum_{k=1}^{d} |X_{i,k} - X_{j,k}|\right))$$
$$lnN + d ln(2\lambda) - \sum_{i=1}^{N} ln \sum_{j=1}^{N} \exp\left(-\frac{1}{\lambda}\sum_{k=1}^{d} |X_{i,k} - X_{j,k}|\right)) \quad (12)$$

In the realm of SCC parameter selection, PMI helps uncover which parameters (X) have the most vital relationship with the compressive and tensile strengths (Y) while considering the influence of other parameters (Z). This approach enables us to identify the most significant parameters contributing to SCC's mechanical properties, leading to more accurate and optimized models for predicting compressive and tensile strengths.

3. RESULT AND DISCUSSIONS

This section explores the results of sensitivity analysis, the creation of AI models, and the testing.

3.1. Sensitivity Analysis

In the realm of SCC, understanding the relationships between input parameters and vital mechanical properties like compressive and tensile strength is pivotal for optimizing material formulations. The correlation matrix gives the first insight into the selection parameters in AI modeling. Matrices 1 and 2 give the correlation between the selected parameters. When analyzing the correlation matrix 1 for CS28, a comprehensive picture emerges regarding the interplay between input parameters and the target strength. Each parameter's correlation coefficient with compressive strength offers valuable information on its impact. The parameter SP demonstrates a positive correlation of 0.68, indicating that as the superplasticizer content increases, CS28 tends to rise. Similarly, PC boasts a correlation of 0.72, indicating that higher powder content is associated with enhanced compressive strength.

Matrix 1.
Correlation matrix for CS28

VARIABLES	SP	PC	PPF	SF	SFD	SFT	VF	CS28
SP	1.00	0.14	0.00	0.00	0.42	-0.36	-0.32	0.68
PC	0.14	1.00	0.02	0.02	0.36	-0.36	-0.44	0.72
PPF	0.00	0.02	1.00	-0.01	-0.67	0.70	0.66	0.16
SF	0.00	0.02	-0.01	1.00	-0.30	0.23	0.31	0.32
SFD	0.42	0.36	-0.67	-0.30	1.00	-0.98	-0.96	0.28
SFT	-0.36	-0.36	0.70	0.23	-0.98	1.00	0.97	-0.25
VF	-0.32	-0.44	0.66	0.31	-0.96	0.97	1.00	-0.26
CS28	0.68	0.72	0.16	0.32	0.28	-0.25	-0.26	1.00

While PPF displays a weaker positive correlation of 0.16, SF exhibits a moderate correlation of 0.32, suggesting that both parameters contribute positively to compressive strength. SFD and SFT highlight corre-

lations of 0.28 and -0.25, respectively, signifying that larger diameter slump flow values are linked to better compressive strength. In contrast, longer slump flow times tend to lower it slightly. VF shows a similar trend with a correlation of -0.26.

Matrix 2.
Correlation matrix for TS28

Variables	SP	PC	PPF	SF	SFD	SFT	VF	TS28
SP	1.00	0.14	0.00	0.00	0.42	-0.36	-0.32	0.71
PC	0.14	1.00	0.02	0.02	0.36	-0.36	-0.44	0.69
PPF	0.00	0.02	1.00	-0.01	-0.67	0.70	0.66	0.21
SF	0.00	0.02	-0.01	1.00	-0.30	0.23	0.31	0.29
SFD	0.42	0.36	-0.67	-0.30	1.00	-0.98	-0.96	0.26
SFT	-0.36	-0.36	0.70	0.23	-0.98	1.00	0.97	-0.23
VF	-0.32	-0.44	0.66	0.31	-0.96	0.97	1.00	-0.25
TS28	0.71	0.69	0.21	0.29	0.26	-0.23	-0.25	1.00

Turning attention to matrix 2 for TS28, the overarching pattern of positive correlations prevails. Most parameters exhibit positive relationships with tensile strength, signifying their potential to influence this mechanical property. SP and PC maintain their influence, with correlations of 0.71 and 0.69, respectively. PPF demonstrates a correlation of 0.21, indicating a moderate impact on tensile strength. SF presents a similar trend with a correlation of 0.29. Interestingly, SFD and SFT remain consistent with their compressive strength relationships, highlighting correlations of 0.26 and -0.23, respectively. Again, VF demonstrates a weak negative correlation of -0.25.

3.2. Input Variable Selection through PMI

The results of the relative importance analysis through PMI for predicting the CS28 and TS28 of SCC using various input variables are shown in Fig. 4. Each row corresponds to a specific variable, and the "Rel_Importance_CS28" and "Rel_Importance_TS28" columns indicate the calculated relative importance values for CS28 and TS28, respectively. For CS28 prediction, the obtained relative importance values provide valuable insights into the significance of each variable. Among the variables, SFD exhibits higher importance with a relative importance value of 0.73. This implies that the SFD parameter has a substantial influence on predicting CS28. The VF parameter follows with a notable relative importance value of 0.68, emphasizing its meaningful contribution to CS28 estimation. Other variables, such as SF, SFT, and PPF, are essential, contributing 0.50, 0.58, and 0.42, respectively. Meanwhile, PC and SP have relatively lower importance values of 0.26 and 0.33, indicating a lesser impact on CS28 prediction.

Turning to TS28 estimation, Fig. 4 reveals the relative importance values of the variables for predicting tensile strength. Like CS28, SFD plays a pivotal role with a high relative importance value of 0.72, indicating its strong influence on TS28 estimation. The VF variable also maintains significance, as indicated by a relative importance value of 0.67. Moreover, SF demonstrates substantial importance with a relative value of 0.48, reinforcing its contribution to predicting TS28. Similarly, SFT and PPF exhibit notable importance values of 0.56 and 0.41, respectively. SP and PC show lower importance values of 0.34 and 0.27, suggesting their comparatively lesser roles in TS28 prediction.

The relative importance values in CS28 and TS28 prediction scenarios provide a clear hierarchy of the variables' contributions. These values guide the prioritization of variables while constructing accurate and efficient AI models for estimating SCC strength. The results underscore the key variables that heavily influence the prediction outcomes, facilitating better decision-making in selecting input parameters and enhancing the interpretability and performance of the AI models in SCC strength estimation.

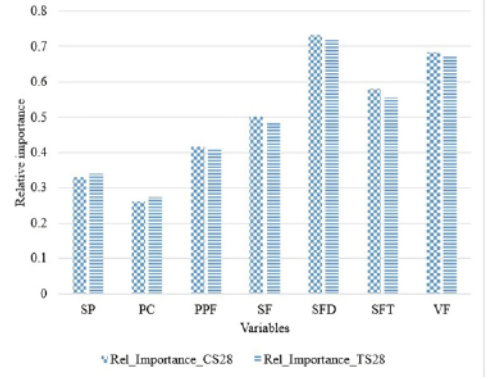

Figure 4.
Relative importance of each parameter

3.3. Gene Expression Programming (GEP)

GEP modeling was done using MATLAB GEP modeling for predicting CS28 and TS28 of SCC. This provides valuable insights into the accuracy and performance of the developed models Eq. 13 and Eq. 14, respectively. For CS28 prediction, the Coefficient of Variation (CV) value of 0.116 indicates the variabili-

ty in the predicted values around the mean. A lower CV suggests that the predicted values are relatively consistent and closely aligned with the actual data points, indicating good model performance in terms of precision and reliability. The Normalized Mean Square Error (NMSE) of 0.517 reflects the extent of the model's accuracy in predicting CS28. A lower NMSE value signifies a better fit between the predicted and actual values. In this case, the NMSE value indicates that the GEP model captures more than half of the variation in the data, implying that the model performs reasonably well in approximating the target CS28 values. The correlated values of the actual and prediction of 0.696 demonstrate the strength of the linear relationship between the predicted and actual CS28 values. A correlation value closer to "1" shows a higher degree of agreement between the model's predictions and the actual data, suggesting that the GEP model accurately represents CS28.

Similarly, for TS28 prediction, the CV value of 0.112 suggests consistent and reliable predictions with relatively low variability around the mean. The lower CV indicates stable model predictions for TS28. The NMSE of 0.376 reflects the accuracy of the TS28 prediction model. With a value less than 0.5, the NMSE indicates a relatively good fit between the predicted and actual TS28 values, signifying the model's capability to capture a substantial portion of the data variation. The correlation of 0.797 between the actual and predicted TS28 values illustrates a robust linear relationship between the two sets of values. This high correlation value implies that the GEP model for TS28 prediction aligns closely with the actual data, indicating the model's ability to estimate TS28 with a high degree of accuracy.

CS28 = ((FA + ((CA1 + SF) * (-0.89))) / ((FA + SP) + (-4.84 – CA2)))

CS28 = CS28 + (FA – ((((SP + Water) – CA2) / (FA / 29.71)) – (-4.69)))

CS28 = CS28 + ((((CA1 - SP) – 78.44) + (SF * 10.50)) / (11.79 – (SF – CA1)))

CS28 = CS28 + ((CA1 / CA2) + (((SF + Water) / 17.16) – (FA - 8.20)))

CS28 = CS28 + ((SF / ((SF * 4.96) – 12.78)) + ((PC / Water) – (-9.60 + (-9.60))))

(13)

TS28 = ((CA2 / (((-0.75 + SF) * CA2) – (PPF * FA))) – 4.94)

TS28 = TS28 + (((CA2 + (SF * -4.22)) / ((SF - Water) * SP)) + 6.59)

TS28 = TS28 + (Water / ((-3.66 - ((3.88 - Water) / 4.00)) - PPF)) (14)

3.4. ANFIS GA model

This innovative model integration aimed to harness the adaptive learning capacity of neuro-fuzzy systems developed in MATLAB, while optimizing the model's parameters using genetic algorithms. Results are presented in Fig. 5 to Fig. 8. During the model development phase, the MSE and RMSE were calculated as 30.8 and 5.53, respectively, for CS28. These numbers express the difference between the strength values that the model predicts and the training data-based strength values. A favorable level of accuracy in reproducing the relationships between the input variables and CS28 was indicated by the relatively low MSE and RMSE values. The CS28 model produced a higher MSE and RMSE of 42.2 and 8.5 when tested against fresh, unexplored data. This result indicates that although the model was proficient at identifying patterns in the training data, it struggled when presented with data outside the parameters of its initial training. The potential overfitting of the model to the training data or the inherent complexity of real-world data may be to blame for this discrepancy. With MSE and RMSE of 0.4 and 0.6, respectively, the model showed even lower errors during model development when focusing on TS28. This encouraging outcome highlights the model's potential to predict tensile strength during its learning phase accurately. However, the MSE and RMSE of the TS28 model increased to 5.4 and 2.4, respectively, during validation. These values remained low, but the difference in performance between development and validation performance points to the need for further validation and fine-tuning to increase the model's ability to generalize to new data.

3.5. Artificial Neural Network

The model's training phase revealed a moderate linear association between the predicted and actual CS28 values, as indicated by the correlation coefficient for CS28 of 0.77. This demonstrated that the model captured a sizable portion of the underlying patterns in the training data. The model successfully reproduced the variations in CS28 based on the input variables as it learned from the training data. After testing the ANN model's performance, the enhanced correlation coefficient of 0.93 revealed a more vital

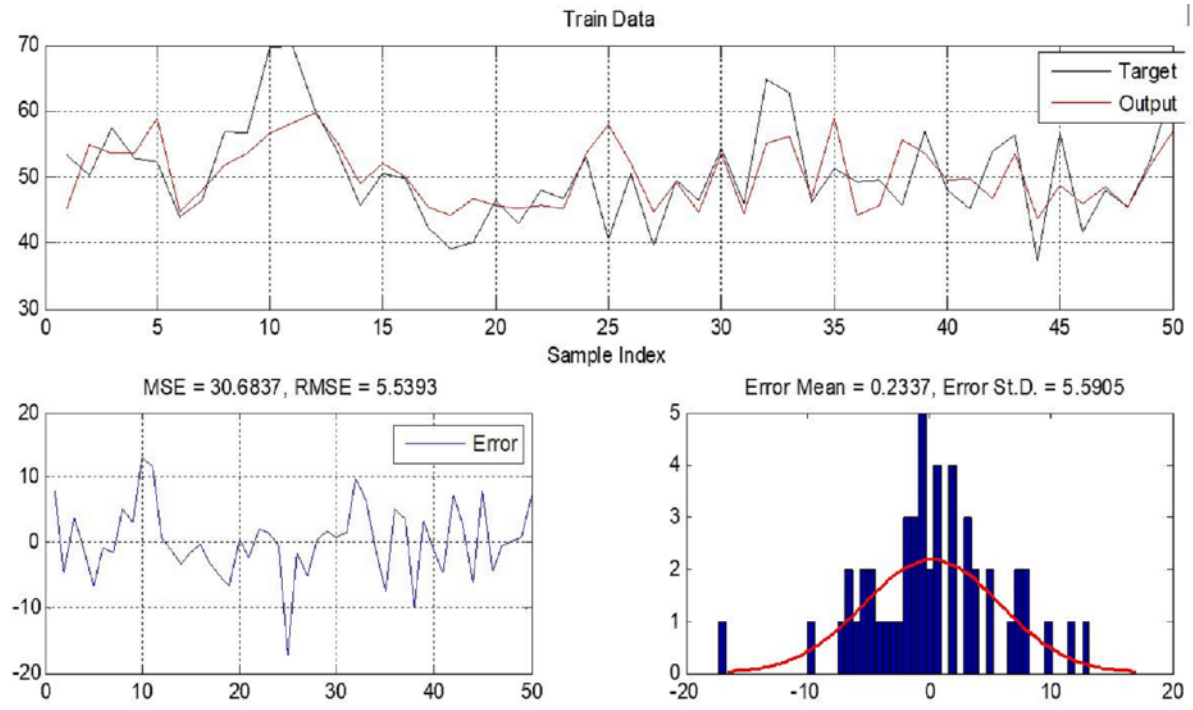

Figure 5.
Training phase results of ANFIS for CS28

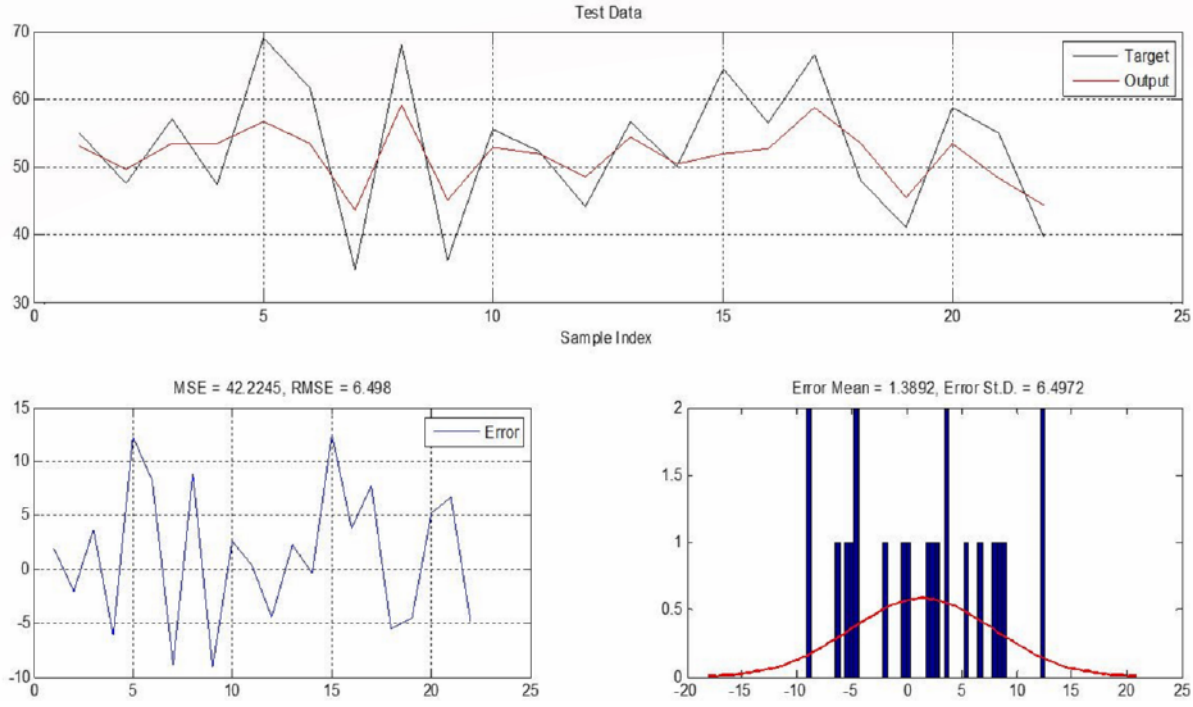

Figure 6.
Testing phase results of ANFIS for CS28

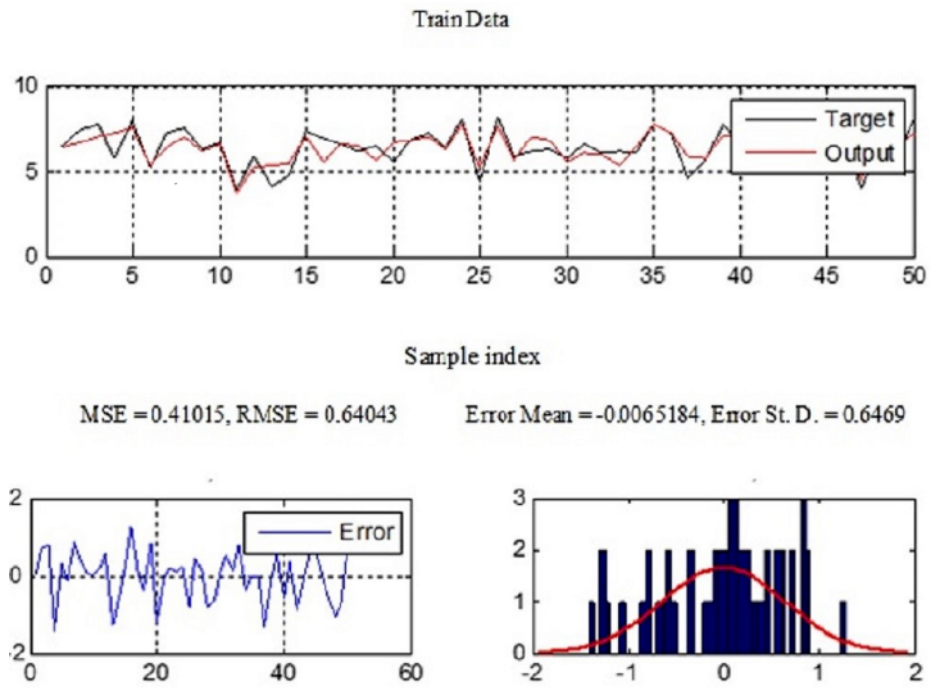

Figure 7.
Training phase results of ANFIS for TS28

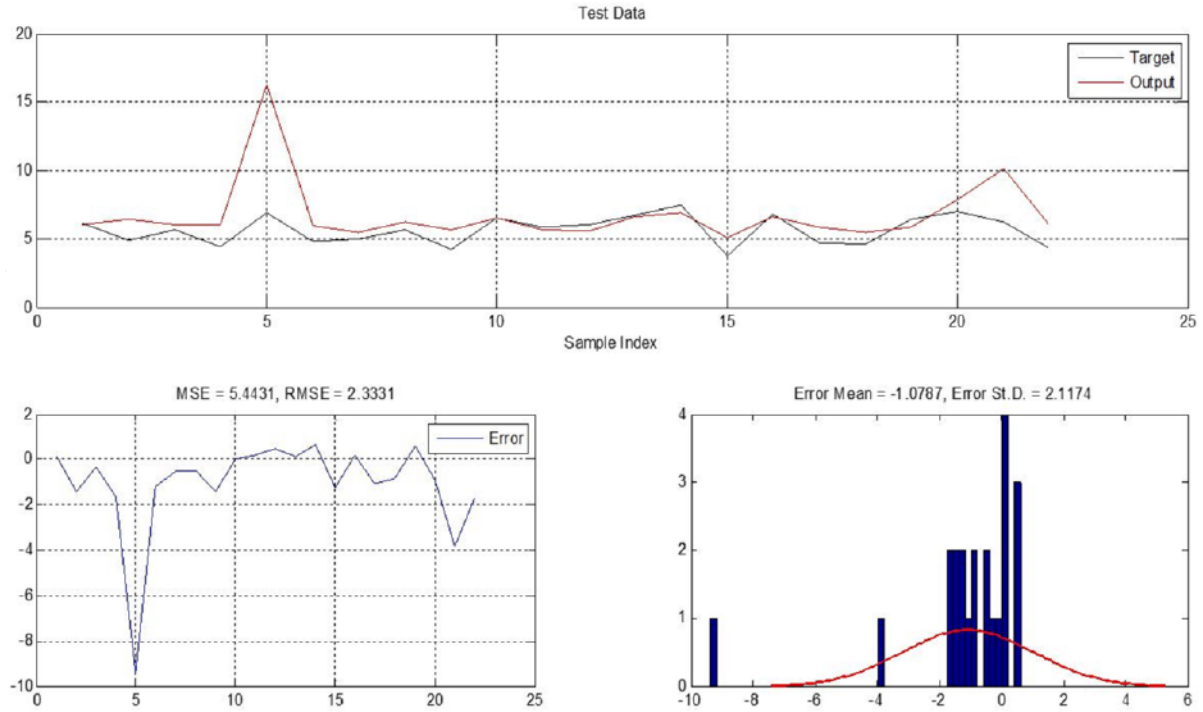

Figure 8.
Testing phase results of ANFIS for TS28

agreement between the predicted and actual CS28 values. With this improvement, the model could generalize beyond its training set and predict CS28 with accuracy for brand-new, untested inputs. The higher correlation during testing demonstrated the ANN model's robustness and generalization abilities, which showed that the ANN model could successfully extrapolate its learning to novel scenarios.

The ANN model's training correlation coefficient of 0.7 for the TS28 prediction indicated a moderate relationship between predicted and actual values. This initial correlation showed that, despite some variability, the model could capture trends in the training data.

The increased correlation coefficient of 0.9 during testing demonstrates the ANN model's improved capability to predict TS28 values correctly. This higher correlation demonstrates the model's ability to handle unknown input variables by showing that it's learning from training translated well to new data. The visual representations of observed versus predicted values for CS28 and TS28 highlighted the model's ability to predict values. Fig. 9 and Fig. 10 demonstrate how the predicted and actual strengths lined up, highlighting the model's effectiveness in estimating SCC properties. Overall, the results of the ANN model's development and testing showed how adept it was at capturing the intricate connections between the input parameters and the corresponding benefits of SCC. The improved correlations during testing for CS28 and TS28 highlighted the model's capability for accurate predictions and strong generalization to new data. This demonstrates the effectiveness of ANN models in calculating SCC strength and their capability to support precise and successful concrete property prediction in practical contexts.

3.6. Support Vector Machines

The SVM model performed admirably during the CS28 prediction task's training and testing phases. The CS28 values anticipated and genuine during preparation showed a healthy level of understanding (0.77-relationship coefficient), demonstrating that the model effectively extricated basic examples from the preparation information. This demonstrated that

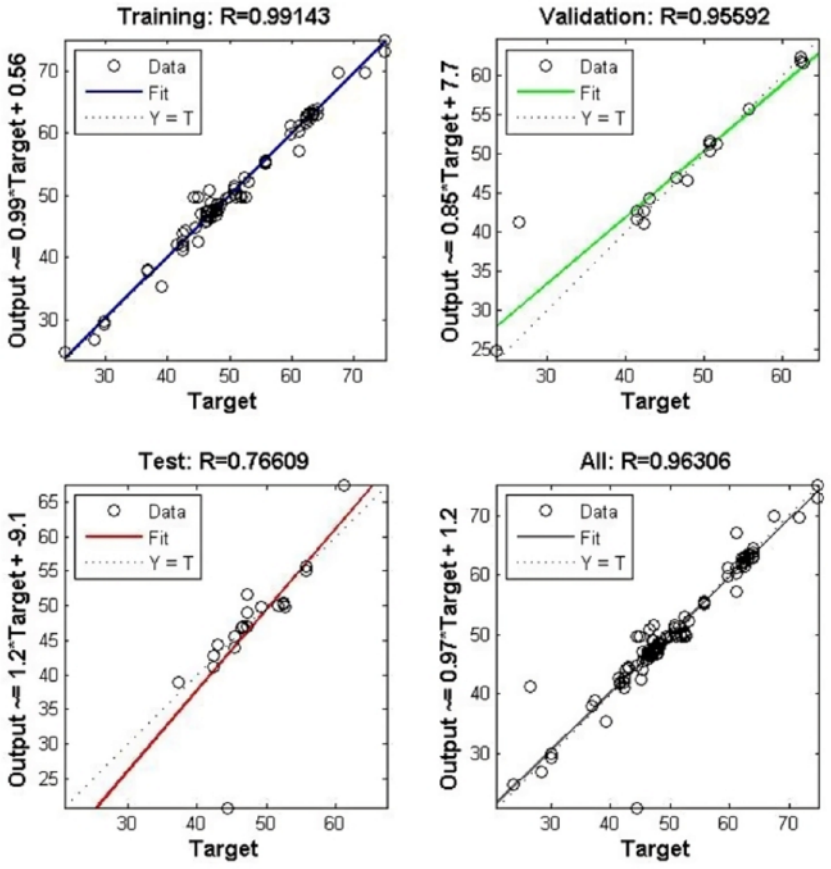

Figure 9.
CS28 results from prediction models

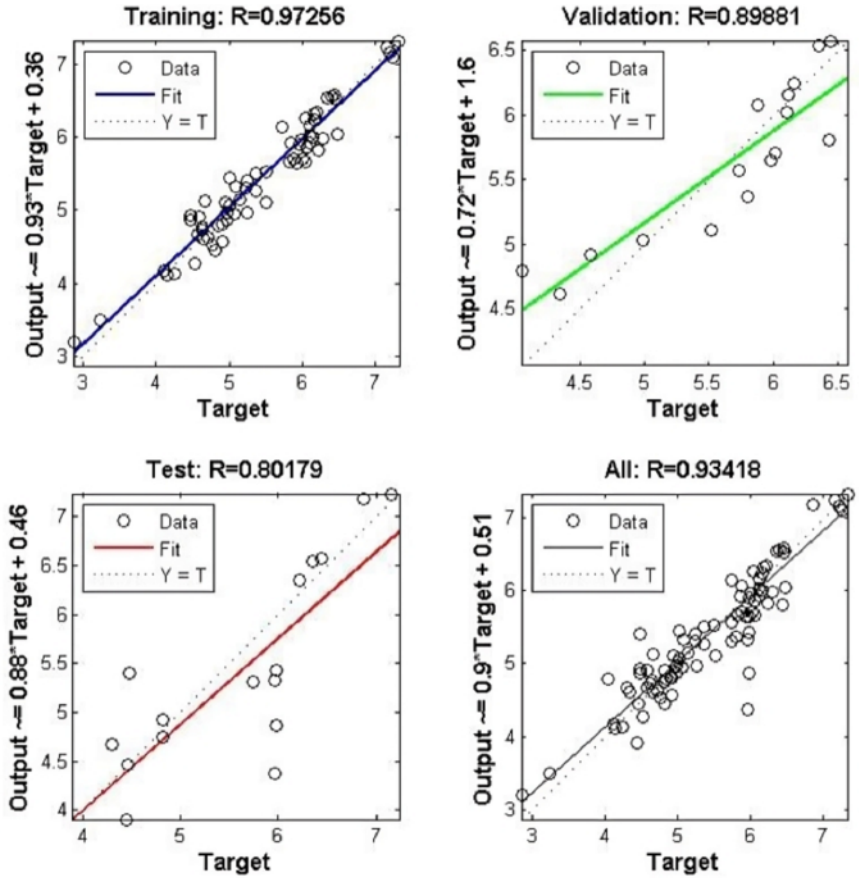

Figure 10.
TS28 results from prediction models

the SVM model correctly identified and replicated the relationships between the input variables and CS28. The SVM model's solid prescient capacities during testing were shown by the relationship coefficient of 0.93, which showed a more significant level of concordance among anticipated and genuine CS28 values. This improvement in connection featured the model's better capacity to sum up new, untested information, as well as its constancy in assessing CS28. The testing predominant connection featured the SVM model's capacity to adjust to various information mixes and make precise forecasts in real situations. The presentation of the SVM model was also empowering for TS28 expectations. The system's ability to identify relationships and trends, although with some variability, was demonstrated by the training data's 0.7 correlation coefficient. The model could construct an establishment for foreseeing TS28 because of the information factors gained from the preparation information. The correlation coefficient of 0.9 indicates that the SVM model performed significantly better during testing, demonstrating its strong generalizability to new data and its capacity to predict TS28 values accurately. This higher connection coefficient featured the model's actual capacity as an exact indicator of TS28 by showing its capacity to extrapolate its learned connections.

3.7. Multiple Linear Regression

The after-effects of the MLR demonstrating the CS28 and TS28 of SCC are shown in Table 4 and Table 5, respectively. These outcomes offer significant bits of knowledge into the accuracy and trustworthiness of the models. The various connection coefficients (Numerous R) for the CS28 expectation created by the MLR model were 0.711514. This worth proposes that the indicator factors (input boundaries) and the CS28 yield have a tolerably certain direct relationship. As per the coefficient of assurance R2 of 0.506253, the model's indicator factors can represent around 50.6% of the variety in CS28. This indicates that the MLR model captures a substantial portion of the variability in CS28, but other factors also contribute to the variation. The adjusted R2 value of 0.452249 reflects the model's

accuracy after considering the number of predictors and degrees of freedom, adjusting for potential overfitting. The standard error 6.190593 represents the average absolute difference between the observed and predicted CS28 values Eq. 15, indicating the model's precision. With 72 observations (Table 1), the model's performance is based on a reasonably sized dataset.

$$CS28 = 92.13 + (0.38 * SP) + (-0.12 * PC) + (1.42 * PPF) + (0.13 * SF) + (0.16 * Water) + (-0.04 * FA) + (-0.01 * CA1) + (0.04 * CA2) \quad (15)$$

For the TS28 prediction, the MLR model demonstrated a higher multiple R2 value of 0.816217, implying a stronger linear relationship between the predictor variables and TS28. The R2 value of 0.66621 indicates that approximately 66.6% of the variability in TS28 can be attributed to the predictor variables employed in the model. This higher R2 suggests that the MLR model is more effective in explaining the variance in TS28 than in CS28. The adjusted R2 value of 0.629702 further validates the model's predictive capability while adjusting for the complexity of the model. The standard error of 0.689796 indicates the average absolute difference between the observed and predicted TS28 values calculated using Eq. 16, indicating the model's precision in predicting TS28. Like the CS28 model, the analysis is based on a dataset containing 72 observations (Table 1).

$$TS28 = 5.1557 - (0.0299 * SP) - (0.0060 * PC) + (0.2266 * PPF) + (0.0160 * SF) + (0.0325 * Water) - (0.0009 * FA) - (0.0037 * CA1) - (0.0037 * CA2) \quad (16)$$

4. COMPARATIVE ANALYSIS

The performance metrics provided offer insights into how different modeling techniques perform in estimating CS28 and TS28 for SCC, as shown in Table 5 and Table 6, respectively.

4.1. Compressive strength at 28 days (CS28)

ANFIS performs moderately with an IOA of 0.50, indicating moderate agreement between observed and predicted values. The AIC of 256.34 suggests that the model may have some complexity. The SS of 0.50 indicates reasonable predictive skill. The SU of 0.01 suggests low uncertainty in the model's predictions.

ANN exhibits a positive IOA of 0.64, indicating a relatively good relation between observed and predicted CS28 values. The AIC of 232.34 indicates a less complex model than ANFIS. The SS of 0.64 suggests that this model has good predictive skills. The SU of 0.29 shows a moderate level of uncertainty in predictions.

SVM outperforms other models with an IOA of 0.96, indicating excellent agreement. The AIC of 68.33 signifies a simpler model. The SS of 0.96 shows strong predictive skill. The SU of 0.93 indicates very low uncertainty.

MLR exhibits moderate agreement with an IOA of 0.51 and an AIC of 256.04. The SS is 0.51, suggesting reasonable predictive skill. The SU is 0.01, indicating low uncertainty.

GEP shows an IOA of 0.62, indicating moderate agreement. The AIC of 159.31 suggests a relatively less complex model. The SS is 0.58, which is reasonable, and the SU is 0.73, indicating moderate uncertainty.

Table 5.
Performance Matrix for CS28

Models	Index of Agreement (IOA)	Akaike Information Criterion (AIC)	Skill Score (SS)	Symmetric Uncertainty (SU)
ANFIS	0.50	256.34	0.50	0.01
ANN	0.64	232.34	0.64	0.29
SVM	0.96	68.33	0.96	0.93
MLR	0.51	256.04	0.51	0.01
GEP	0.62	159.31	0.58	0.73

4.2. Tensile strength at 28 days (TS28)

ANFIS performs well with an IOA of 0.67, indicating good agreement. The negative AIC (-59.96) suggests a relatively simple model. The SS of 0.67 indicates vital predictive skill, while the SU of 0.33 signifies moderate uncertainty.

ANN exhibits negative IOA (-0.54), indicating poor agreement. The positive AIC (50.01) suggests model complexity. The negative SS (-0.54) indicates poor predictive skill, and the SU of -2.07 suggests high uncertainty.

SVM shows good performance with an IOA of 0.81, indicating substantial agreement. The negative AIC (-99.25) suggests model simplicity. The SS of 0.81 reflects strong predictive skill, and the SU of 0.61 indicates moderate uncertainty.

MLR performs well with an IOA of 0.87, indicating excellent agreement. The negative AIC (-127.64) suggests a simple model. The SS of 0.87 indicates strong predictive skill, and the SU of 0.74 signifies moderate uncertainty.

GEP achieves an IOA of 0.62, indicating moderate agreement. The negative AIC (-51.32) suggests a relatively simple model. The SS is 0.62, which is reasonable, and the SU of 0.25 indicates moderate uncertainty.

SVM consistently performs well for CS28 and TS28, with high agreement, strong predictive skills, and low uncertainty. MLR also performs well for both properties. ANN shows good performance for CS28 but struggles with TS28, while ANFIS exhibits good performance for TS28 but moderate performance for CS28. GEP's performance is moderate for both properties.

Table 6.
Performance Matrix for TS28

Models	Index of Agreement (IOA)	Akaike Information Criterion (AIC)	Skill Score (SS)	Symmetric Uncertainty (SU)
ANFIS	0.67	-59.96	0.67	0.33
ANN	-0.54	50.01	-0.54	-2.07
SVM	0.81	-99.25	0.81	0.61
MLR	0.87	-127.64	0.87	0.74
GEP	0.62	-51.32	0.62	0.25

5. CONCLUSIONS

This study primarily focuses on the estimation of CS28 and TS28 of SCC, considering their importance for the assessment of structural integrity and long-term performance. Citing the limitation of conventionally used methods, several advanced techniques such as AI techniques, SVM, ANN, ANFIS-GA, GEP, and MLR were employed to develop predictive models, and the following conclusions were made during the study.

- The results obtained from the study established the AI's superiority over conventional methods, particularly evident in SVM, ANN, and ANFIS-GA models, which exhibited excellent predictive accuracy and robust generalization capabilities.
- Partial Mutual Information (PMI) played a crucial role in the process of identifying the most influential parameters, including superplasticizer, powder content, PP fibre, steel fibre, slump flow (Diameter), slump flow (sec), and V-funnel (sec) and these were found to influence the prediction of CS28 and TS28 significantly.
- The Support Vector Machine is substantiated as the most efficient, reliable, and exact model regarding the CS28 prediction. A remarkable degree of connection of 0.96 and expertise score of 0.96 was accomplished by SVM, exhibiting the technique's ability to gauge CS28 in SCC accurately. Henceforth, it is a powerful tool for reliable prediction of this crucial parameter for designing durable and safe concrete structures.
- In addition, ANN and ANFIS-GA have also exhibited a reasonable prediction of CS28 parameters with a notable correlation of 0.64 and 0.50 and a Skill Score of 0.64 and 0.50, respectively. Further, ANN presents a convincing alternative to SVM, and its ability to capture complex relationships within the data makes it a valuable option.
- In the TS28 prediction, it is inferred that both MLR and SVM models demonstrated excellent results with degrees of connection of 0.81 and 0.87 and expertise scores of 0.81 and 0.87, thus exhibiting strong agreement with actual results and highlighting their potential for accurate predictions.

6. FUTURE SCOPE

The study holds numerous avenues pertinent to enhancing the understanding and prediction of SCC characteristics through various experimental and modeling techniques. Here are some potential future scopes:

- Optimizing and fine-tuning the existing predictive models, especially the SVM, ANN, and ANFIS-GA models, to achieve even higher accuracy in estimating compressive and tensile strengths over a wide variety of mixed designs.
- Extend to a broader range of parameters influencing the properties of SCC, such as curing conditions, type and content of supplementary cementitious materials, and environmental conditions, to develop comprehensive predictive models.
- Exploration of the application of predictive models to estimate dynamic properties of SCC and understanding the long-term performance and durability for the practical implementation of SCC in construction projects.

ACKNOWLEDGMENT

The authors acknowledge the support from Management, Principal SVKMs Institute of Technology, Dhule, India. This research work has no funding support.

CONFLICT OF INTEREST

The authors declare no conflict of interest.

REFERENCES

[1] Zongjin, L. (2011). Advanced concrete technology. New Jersey: John Wiley and Sons Ltd. ISBN 9780470437438.

[2] De Schutter, G., Bartos, P. J., Domone, P., & Gibbs, J. (2008). Self-compacting concrete, (Vol. 288). Caithness: Whittles Publishing.

[3] Li, H., Yin, J., Yan, P., Sun, H., and Wan, Q. (2020). Experimental investigation on the mechanical properties of self-compacting concrete under uniaxial and trial stress. *Materials, 13*(8), 1830.

[4] Boukendakdji O, Kadri EH, Kenai S (2012) Effects of granulated blast furnace slag and superplasticizer type on the fresh properties and compressive strength of self-compacting concrete. *Constr. Build Mater*. 34, 583–590.

[5] Zhang, X., Luo, Y., Wang, L., Zhang, J., Wu, W., & Yang, C. (2018). Flexural strengthening of damaged RC T-beams using self-compacting concrete jacketing under different sustaining loads. *Construction and Building Materials*, 172, 185–195. doi:10.1016/j.conbuildmat.2018.03.245.

[6] Chalioris, C. E., & Pourzitidis, C. N. (2012). Rehabilitation of shear-damaged reinforced concrete beams using self-compacting concrete jacketing. ISRN Civil Engineering, 816107. doi:10.5402/2012/816107.

[7] Sucharda, O., Brozovsky, J., & Mikolasek, D. (2014). Numerical modeling and bearing capacity of reinforced concrete beams. Key Engineering Materials, 281–284. doi:10.4028/www.scientific.net/KEM.577-578.281

[8] Czarnecki, S., Shariq, M., Nikoo, M., & Sadowski, Ł. (2021). An intelligent model for the prediction of the compressive strength of cementitious composites with ground granulated blast furnace slag based on ultrasonic pulse velocity measurements. Measurement: Journal of the International Measurement Confederation, 172, 108951. doi:10.1016/j.measurement.2020.108951.

[9] Nicoara, A. I., Stoica, A. E., Vrabec, M., Šmuc Rogan, N., Sturm, S., Ow-Yang, C., & Vasile, B. S. (2020). End-of-life materials are used as supplementary cementitious materials in the concrete industry. Materials, 13, 1954. doi: 10.3390/ma13081954.

[10] EN British Standard. 450-1, Fly Ash for Concrete-Definition, Specifications, and Conformity Criteria. British Standards Institution; London, UK, 2012.

[11] Asteris, P. G., & Kolovos, K. G. (2019). Self-compacting concrete strength prediction using surrogate models. *Neural Computing and Applications, 31*(1), 409–424.

[12] Rajakarunakaran, S. A., Lourdu, A. R., Muthusamy, S., Panchal, H., Alrubaie, A. J., Jaber, M. M & Ali, S. H. M. (2022). Prediction of strength and analysis in self-compacting concrete using machine learning based regression techniques. Advances in Engineering Software, 173, 103267.

[13] Dutta, S., Murthy, A. R., Kim, D., & Samui, P. (2017). Prediction of Compressive Strength of Self-Compacting Concrete Using Intelligent Computational Modeling. *Computers, Materials & Continua, 53*(2).

[14] Dutta, S., Samui, P., & Kim, D. (2018). Comparison of machine learning techniques to predict the compressive strength of concrete. *Comput. Concr. 21*(4), 463–470.

[15] Sri Rama Chand, M., Rathish Kumar, P., Swamy Naga Ratna Giri, P., Rajesh Kumar, G., & Krishna Rao, M. V. (2016). Influence of paraffin wax as a self-curing compound in self-compacting concretes. *Advances in Cement Research, 28*(2), 110–120.

[16] Madduru, Sri Rama & Pancharathi, Rathish & Giri, P Swamy & G., Rajesh. (2018). Performance studies on self-compacting concrete with self-curing chemicals. *Indian Concrete Journal*. 92. 24–30.

[17] Chand, M. S. R., Giri, P. S. N. R., Kumar, P. R., Kumar, G. R., & Raveena, C. (2016). Effect of self-curing chemicals in self-compacting mortars. *Construction and Building Materials*, 107, 356–364.

[18] Sri Rama Chand, M., Rathish Kumar, P., Swamy Naga Ratna Giri, P., & Rajesh Kumar, G. (2018). Performance and microstructure characteristics of self-curing self-compacting concrete. *Advances in Cement Research, 30*(10), 451–468.

[19] Gamil, Y., Nilimaa, J., Najeh, T., & Cwirzen, A. (2023). Formwork pressure prediction in cast-in-place self-compacting concrete using deep learning. *Automation in Construction*, 151, 104869.

[20] Farooq, F., Czarnecki, S., Niewiadomski, P., Aslam, F., Abdul-Jabbar, H., Ostrowski, K. A., Śliwa-Wieczorek, K. (2021). A comparative study for the prediction of the compressive strength of self-compacting concrete modified with fly ash. *Materials, 14*(17), 4934. MDPI AG. Retrieved from http://dx.doi.org/10.3390/ma14174934.

[21] Siddique, R., Aggarwal, P., Aggarwal, Y. (2011). Prediction of compressive strength of self-compacting concrete containing bottom ash using artificial neural networks. *Advances in Engineering Software, 42*(11), 780–786.

[22] Saha, P., Debnath, P., Thomas, P. (2020). Prediction of fresh and hardened properties of self-compacting concrete using support vector regression approach. *Neural Computing and Applications, 32*(17), 7995–8010.

[23] Hoang, N. D. (2022). Machine learning-based estimation of the compressive strength of self-compacting concrete: A multi-dataset study. *Mathematics, 10*(20), 3771. Retrieved from http://dx.doi.org/10.3390/math10203771.

[24] Prasad, B. K. R., Eskandari H., Reddy B. V. V. (2009). Prediction of compressive strength of SCC and HPC with high volume fly ash using ANN. *Construction and Building Materials, 23*(1), 117–128.

[25] Mai, H. V. T., Nguyen, M. H., Trinh, S. H., & Ly, H. B. (2023). Optimization of machine learning models for predicting the compressive strength of fiber-reinforced self-compacting concrete. *Frontiers of Structural and Civil Engineering, 17*(2), 284–305.

[26] Pallapothu, S. N. R. G., Pancharathi, R. K., & Janib, R. (2023). Predicting concrete strength through packing density using machine learning models. *Engineering Applications of Artificial Intelligence*, 126, 107177.

[27] Candida Ferreria (2001). Gene expression programming: a new adaptive algorithm for solving problems, *Complex Systems, 13*(2), 87–129.

[28] Vakhshouri, B., & Nejadi, S. (2018). Prediction of compressive strength of self-compacting concrete by ANFIS models. *Neurocomputing*, 280, 13–22.

[29] Al-Mughanam, T., Aldhyani, T. H., Alsubari, B., & Al-Yaari, M. (2020). Modeling of compressive strength of sustainable self-compacting concrete incorporating treated palm oil fuel ash using artificial neural network. *Sustainability, 12*(22), 9322.

[30] Boser, B.E., Guyon, I.M., and Vapnik, V.N. (1992). A training algorithm for optional margin classifiers. Proceedings of the Fifth Annual Workshop on Computational Learning Theory, Pittsburgh, 144–152.

[31] Çevik, A., Kurtoğlu, A. E., Bilgehan, M., Gülşan, M. E., & Albegmprli, H. M. (2015). Support vector machines in structural engineering: a review. *Journal of Civil Engineering and Management, 21*(3), 261–281.

[32] Armstrong, N., Sutton, G. J., & Hibbert, D. B. (2019). Estimating probability density functions using a combined maximum entropy moments and Bayesian method. *Theory and numerical examples. Metrologia, 56*(1), 015019.

[33] Sharma Ashish (2000). Seasonal to interannual rainfall probabilistic forecast for improved water supply management: part 1-A strategy for system predictor identification. *Journal of Hydrology, 239*(1), 232–239.